Contract No:

This document was prepared in conjunction with work accomplished under Contract No. 89303321CEM000080 with the U.S. Department of Energy (DOE) Office of Environmental Management (EM).

Disclaimer:

This work was prepared under an agreement with and funded by the U.S. Government. Neither the U.S. Government or its employees, nor any of its contractors, subcontractors or their employees, makes any express or implied:

1) warranty or assumes any legal liability for the accuracy, completeness, or for the use or results of such use of any information, product, or process disclosed; or
2) representation that such use or results of such use would not infringe privately owned rights; or
3) endorsement or recommendation of any specifically identified commercial product, process, or service.

Any views and opinions of authors expressed in this work do not necessarily state or reflect those of the United States Government, or its contractors, or subcontractors.

Software Testing to Upgrade M-Star Software for Safety and Waste Form Affecting Applications

S. R. Noble and M. R. Poirier

Savannah River National Laboratory
Aiken, SC 29808

Savannah River Mission Completion (SRMC) currently manages the risk for retained hydrogen in the Defense Waste Processing Facility (DWPF) vessels by implementing a Retained Hydrogen Program. The current program relies on Sludge Batch (SB) 8 Gas Chromatograph data and on conservative assumptions concerning gas release and retention to determine allowable vessel Quiescent time (Q-time).

The authors identified M-Star® CFD as a software that could simulate processes such as fluid flow, heat transfer, species transport, chemical reactions, particle transport, and retained hydrogen gas release. Preliminary simulation results suggest that more realistic assumptions on gas retention and release may be feasible for the DWPF retained hydrogen program. Because of the desire to use the M-Star® software to perform analyses that support nuclear safety, SRMC has requested Savannah River National Laboratory (SRNL) to upgrade the software classification level of M-Star® CFD from level D to level B to perform analyses that support nuclear safety.

To upgrade the M-Star® software from level D to level B, functional testing of the software was performed. Three groups of test problems were selected to validate the capability of the software to represent the physical phenomena characteristic of Savannah River Site (SRS) applications. They are:

- Group 1: Simple, well-defined, classical problems for which analytical solutions exist. These problems are solid particle settling in a liquid, gas bubble rise in a liquid, laminar flow in a pipe, and laminar flow of a Bingham plastic fluid in a pipe. The results from the M-Star® simulations were within 10% of the analytical solution.
- Group 2: Complex problems for which analytical solutions are difficult to obtain or do not exist. For these problems, simulation results were validated through comparisons with documented solutions or experimental data. These problems are determining the impeller power number in an impeller mixed tank, calculating the velocity profile with turbulent flow in a pipe, calculating the pressure drop during turbulent flow in a pipe, and calculating the velocity profile in a turbulent free jet. The results from the M-Star® simulations were within 20% of the established solutions.
- Group 3: Complex problems which are specific to the application of interest. The test problems are miscible liquid blending in a jet mixed tank, miscible liquid blending in an impeller mixed tank containing a non-Newtonian fluid, cavern mixing with an impeller in a tank containing a non-Newtonian fluid, and gas release from a Bingham plastic fluid in an impeller mixed tank. The results from the M-Star® simulations were within 30% of the experimental data.

INTRODUCTION

Savannah River Mission Completion (SRMC) currently manages the risk for retained hydrogen in the Defense Waste Processing Facility (DWPF) vessels by implementing a Retained Hydrogen Program. The current program relies on Sludge Batch (SB) 8 Gas Chromatograph data and on conservative assumptions concerning gas release and retention to determine allowable vessel Quiescent time (Q-time).[1, 2]

M-Star® CFD is a multi-physics modeling package used to simulate fluid flow, heat transfer, species transport, chemical reactions, particle transport, and rigid-body dynamics. M-Star® CFD contains three primary components: M-Star® Build, M-Star® Solve and M-Star® Post. M-Star® Build is a graphical interface used to prepare models and specify simulation parameters. M-Star® Solve uses input files

generated from the interface to execute the simulation. M-Star® Post renders and plots the data generated by the solver.[1]

Savannah River National Laboratory (SRNL) is testing and verifying the software so that it can be used to perform simulations that support nuclear safety.

SOFTWARE TESTING

The test problems were selected based on the fact that analytical solutions (or excellent approximations) exist that definitively establish the code accuracy, capability, and the resulting impact that mesh and control parameter settings have on accuracy. Three groups of test problems are described to validate the capability of the software to represent the physical phenomena characteristic of Savannah River Site (SRS) applications. They are:

Group 1: Simple, well-defined, classical problems for which analytical solutions exist.

Group 2: Complex problems for which analytical solutions are difficult to obtain or don't exist. For these problems, code results are validated through comparisons with documented solutions or experimental data.

Group 3: Complex problems which are specific to the application of interest.

RESULTS AND DISCUSSION

Group 1 Problems

For Group 1, the authors selected four problems to simulate. These problems are solid particle settling in a liquid, gas bubble rise in a liquid, laminar flow in a pipe, and laminar flow of a Bingham plastic fluid in a pipe. The acceptance criterion for these problems is that the results of the M-Star simulations are within 10% of the analytical solution.

Particle Settling

Solid particle settling rates can be calculated by Stokes Law and other particle settling equations, which are described by equations [1] - [5]

$$v_s = g(s-1)d_p^2/18\nu \quad \text{for } Re_p < 1 \qquad [1]$$

$$v_s = g^{0.8}(s-1)^{0.8}d_p^{1.4}/10\nu^{0.6} \quad \text{for } 1 < Re_p < 50 \qquad [2]$$

$$v_s = g^{0.6}(s-1)^{0.6}d_p^{0.8}/2.13\nu^{0.2} \quad \text{for } 50 < Re_p < 1620 \qquad [3]$$

$$v_s = 1.83\, g^{0.5}(s-1)^{0.5}d_p^{0.5}/\nu^0 \quad \text{for } Re_p > 1620 \qquad [4]$$

$$Re_p = d_p v_s/\nu \qquad [5]$$

where v_s is the settling velocity, g is the acceleration due to gravity, s is the ratio of particle and fluid densities (s = particle density/fluid density), d_p is the particle diameter, ν is the fluid kinematic viscosity ($\nu=\mu/\rho$), μ is the fluid viscosity, ρ is the fluid density, and Re_p is the particle Reynolds number.[3]

M-Star® simulations were performed using particles of varying size, and a density of 2.5 g/mL. The liquid density was 1.0 g/mL, and the liquid viscosity was 1.0 cP. Figure 1 a shows the comparison between the M-Star® simulations and equations [1] – [5]. In the region where Stokes Law describes particle settling (particle size less than 107 micron), the M-Star® calculated settling rate is within 1% of the Stokes Law prediction. With a particle size of 200 – 500 microns, the M-Star® calculated settling rate agrees with equation [2] to within 15%. Equation [1] is an analytical solution for particle settling, while equations [2] – [4] are empirical correlations, so a larger difference would be expected in those comparisons, and an

[1] mstarcfd.com

acceptance criterion of ±20% would be appropriate. The test of the M-Star® software at simulating particle settling is determined to be successful.

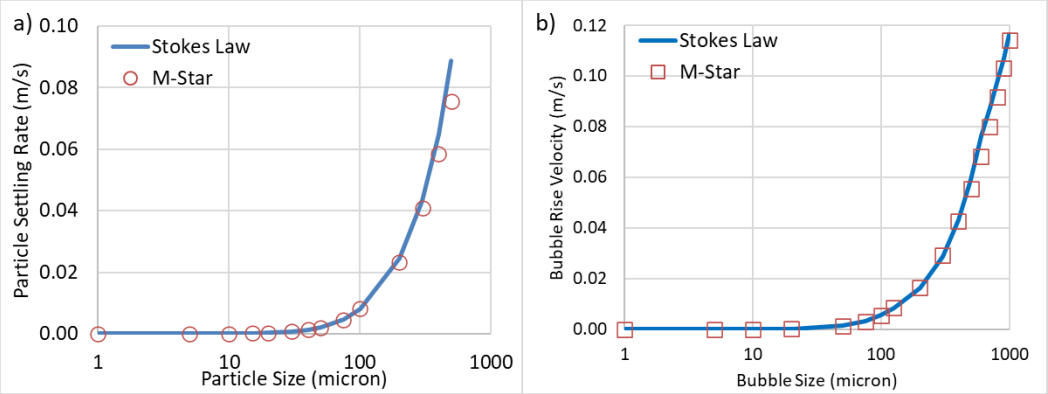

Figure 1. Comparison of M-Star Predicted Particle Settling (a) and Bubble Rise (b) with Stokes Law

Bubble Rise

The rise of a gas bubble in a liquid can also be calculated with equations [1] - [5] using the bubble size and density instead of the particle size and density. The bubble density was 0.001 g/mL, the liquid density was 1.0 g/mL, and the liquid viscosity was 1 cP. The authors made the following assumptions for these simulations: the gas bubbles are spherical, no transfer of material occurs between the bubble and the liquid, no internal recirculation occurs within the bubble, and no slip occurs between the liquid and the bubble. Figure 1 b shows the comparison between the M-Star® simulations and equations [1] – [5]. In the region where Stokes Law describes the bubble rise (bubble size less than 123 micron), the M-Star® calculated rise rate is within 1% of the Stokes Law prediction. With a bubble size of 1– 400 microns, the M-Star calculated rise rate agrees with equation [2] to within 1%, and with a bubble size of 400 – 1,000 microns, the M-Star calculated rise rates agree with equation [3] to within 12%. Given that Stokes Law is not applicable for this range of bubble size and comparisons are with empirical correlations, an acceptance criterion of ±20% is appropriate. The test of the M-Star® software at simulating bubble rise is determined to be successful.

Laminar Pipe Flow

The velocity profile of a laminar flow in a pipe was calculated and compared with fluid dynamics theory. The analytical solution for the radial velocity profile is described by equation [6]

$$V(r) = V_{max} (1 - r^2/R^2) \quad [6]$$

where v(r) is the axial velocity as a function of radial position, v_{max} is the maximum or centerline velocity, r is the radial position, and R is the pipe radius.[4] The following parameters were used for this simulation: a liquid density of 1 g/mL, a liquid viscosity of 1 cP, a bulk velocity of 0.01 m/s, a pipe diameter of 0.1 m, and a pipe length of 10 m. The Reynold number is 1,000. Figure 2 shows the velocity profile described by equation [6]. Some difference is observed in the velocity near the wall. The reason for this difference is that M-Star calculates the velocity in a lattice volume rather than at a single point. The zero velocity boundary condition occurs in the lattice volume near the wall rather than at the wall. As the lattice spacing decreases, the difference becomes smaller. The available computers limited the number of lattice points across the pipe diameter in the simulation. The agreement between the M-Star® simulation and the analytical solution is very good, with a difference of less than 5%. The test of the M-Star® software at simulating laminar pipe flow is determined to be successful.

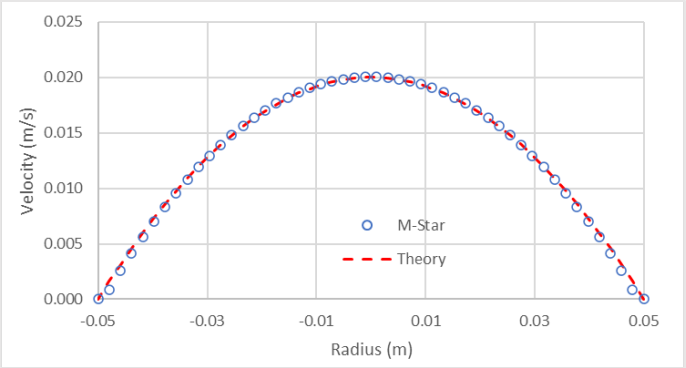

Figure 2. Axial Velocity Profile across a Pipe Diameter in Laminar Flow

Laminar Bingham Plastic Pipe Flow

Under laminar flow conditions, a Bingham plastic fluid has a flat, plug flow in the center of the pipe, and a varying velocity profile near the pipe wall. The radius of the plug flow region is described by equation [7]

$$r_{plug} = R\ \tau_y/\tau_w \quad [7]$$

where r_{plug} is the radius of the plug flow region, R is the pipe radius, τ_y is the fluid yield stress, and τ_w is the wall shear stress. When the radial position is less than r_{plug}, the velocity is described by equation [8]

$$V_{plug} = (R\tau_w/\mu_B)(1 - \tau_y/\tau_w)^2 \quad [8]$$

where μ_B is the consistency or plastic viscosity. When the radial position is greater than r_{plug}, the velocity is described by equation [9].[5]

$$v = (R\tau_w/\mu_B)\,[1 - (r/R)^2] - (R\tau_y/\mu_B)\,(1 - r/R) \quad [9]$$

The velocity profile from a simulation of laminar flow of a Bingham plastic fluid in a pipe was compared with the predictions of equations [7] – [9]. The following parameters were used for this simulation: a liquid density of 1 g/mL, a yield stress of 1 Pa, a plastic viscosity of 1,000 cP, a bulk velocity of 1 m/s, a pipe diameter of 0.1 m, and a pipe length of 2 m. The Reynold number is 100. Figure 3 shows the velocity profiles for laminar flow of a Bingham plastic fluid in a pipe calculated using equations [7] – [9], as well as the velocity profile from the M-Star® Simulation in yield stresses of 1 Pa, 10 Pa, and 50 Pa. For a 1 Pa yield stress solving equations [7] – [9], the radius of the plug flow region (r_{plug}) is 0.000615. In the M-Star® simulations, the normalized radius of the plug is 0.000625. The plug velocity was 1.970 m/s in the M-Star® simulations and 1.983 m/s in the analytical solution, a difference of less than 1%. The normalized velocity (v/v_{plug}) was 99% at 0.0056 meters in the M-Star® simulation and in the analytical solution. The normalized velocity (v/v_{plug}) was 90% at 0.0163 meters in the M-Star simulation and in the analytical solution. The pressure drop was was 3297 Pa/m in the M-Star® simulation and 3251 Pa/m in the analytical solution, a difference of less than 1.5%.

Table I compares the axial velocity from the M-Star simulations with the axial velocity from the analytical solution at select radial positions. In all cases but one, the velocities are within 10%. In one case, the difference is 11%. Table II shows the M-Star® calculated axial pressure drop for the 1 Pa, 10 Pa, and 50 Pa fluids compared with the analytical solution. The M-Star® calculated pressure drop is within 6% of the analytical solution.These results show that the M-Star® software can simulate the flow of a Bingham plastic fluid in a pipe. The test of the M-Star® software at simulating Bingham plastic flow in a pipe is determined to be successful.

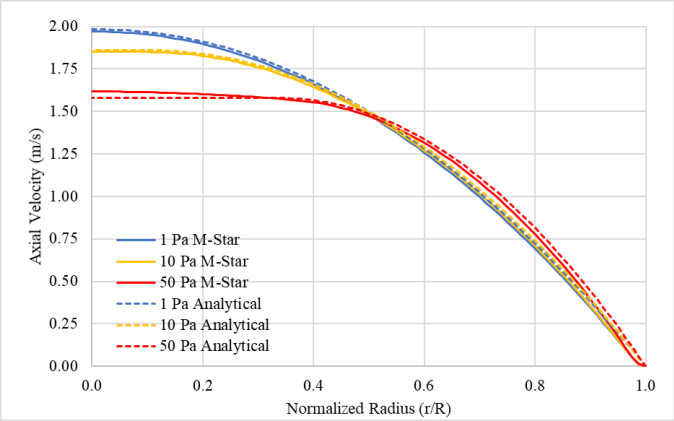

Figure 3. Axial Velocity Across a Pipe Radius during Flow of a Bingham plastic

Table I. Comparison of M-Star Simulations with Analytical Solution

	$V_{M\text{-}Star}/V_{Analytical}$		
r/R	1 Pa	10 Pa	50 Pa
0.1	0.99	0.99	1.02
0.25	0.99	0.99	1.01
0.5	0.99	0.99	0.99
0.75	0.97	0.97	0.97
0.9	0.91	0.9	0.89

Table II. Axial Pressure Drop for Bingham Plastic Pipe Flow

Yield Stress (Pa)	1	10	50
$\Delta P_{M\text{-}Star}$ (Pa/m)	3297	106,997	110,200
$\Delta P_{Analytical}$ (Pa/m)	3251	103,215	104,283
Ratio	1.01	1.04	1.06

Group 2 Problems

For Group 2, the authors selected four problems to simulate. These problems are determining the impeller power number in an impeller mixed tank, calculating the velocity profile with turbulent flow in a pipe, calculating the pressure drop during turbulent flow in a pipe, and calculating the velocity profile in a turbulent free jet. The acceptance criterion for these problems is that the results of the M-Star® simulations are within 20% of the established solution.

Power Number

Determining an impeller power number is an important application for mixing equipment suppliers. Knowing the power number allows one to determine the power draw and size the motor for the agitator. It also allows for optimizing the impeller diameter and impeller speed. In addition, many correlations for parameters such as blend time, cavern diameter, gas bubble size, liquid droplet size, and mass transfer coefficient depend on the agitator power.[6]

Simulations with rotating impellers were performed to validate the predicted impeller torque against measured data over a range of Reynolds numbers. Each test case considered a single Rushton, pitch blade, or hydrofoil impeller in a baffled 1 m diameter tank with an impeller diameter of 0.5 m. The impellers were centered in the vessel with a one-diameter off-bottom clearance. The viscosity of the fluid was assumed to be constant but varied between simulations to sweep over a range Reynolds numbers. All simulations were performed using a lattice spacing of 250 points across the vessel diameter.

In Figure 4, we show the power number from the M-Star® simulations and the literature as a function of Reynolds number for all three impellers. In each system, the Reynolds number Re is defined by:

$$Re = \frac{ND^2}{\nu} \quad [10]$$

where N is the impeller speed (in revolutions per second) and D is the impeller diameter. Likewise, the power number N_p for each system is defined from:

$$N_p = \frac{2\pi\tau N}{\rho N^3 D^5} \quad [11]$$

where τ is the torque on the impeller. The general trends are consistent between the two data sets: at low Reynolds numbers (Re<100), the power number increases exponentially with decreasing Reynolds number. At high Reynolds numbers (Re>10,000), the power number of each impeller becomes constant. Between these two extremes, around Re=1,000, there is a transitional regime with a small local minimum in power draw. Across the full range of Reynolds number and impeller shapes, the power numbers predicted from the simulations are within 13% of the measured values.

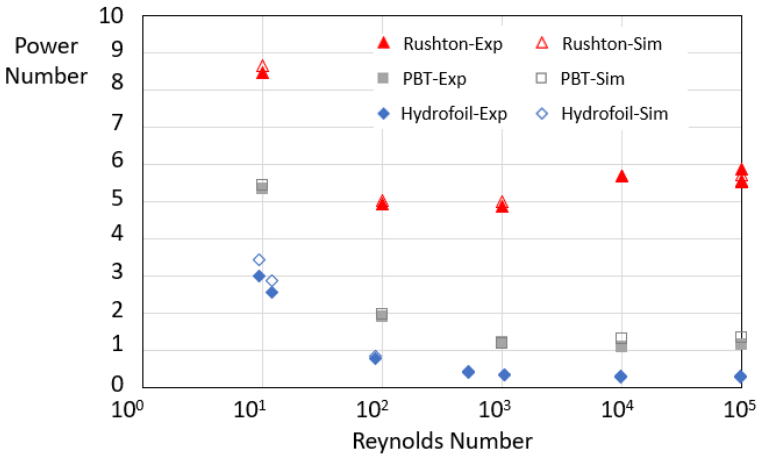

Figure 4. Simulation predicted (Sim) versus experimentally measured (Exp) power numbers for multiple impellers across a range of Reynolds numbers

Because many processes at SRS involve the mixing of non-Newtonian fluids with impellers. Additional tests of the M-Star® software were performed to calculate the power number of impellers in this application. Nagata et al measured the power number of a number of impellers during the mixing of Bingham plastic fluids.[7] Their data set included Rushton impellers and flat blade paddles. The fluid density was 1330 kg/m^3, the fluid yield stress was 15 Pa, and the fluid consistency was 40 cP. The turbine rotated at 130 rpm. These parameters were selected to match the design of the DWPF SME. Figure 5 shows the general layout of the vessels used in the every mixing simulation with the impeller being a 6-blade paddle or Rushton turbine. Simulations of mixing of Bingham plastic fluids under turbulent conditions as those used by Nagata et al were performed, and the power numbers are shown in Table III. The power numbers from the M-Star® simulations agree with the data of Nagata et al within 5%. The test of the M-Star® software at determining the impeller power number during impeller mixing of Newtonian and Bingham plastic fluids is determined to be successful.

Table III. Impeller Power Number during Mixing of Non-Newtonian Fluids

Impeller	Nagata et al	M-Star	Ratio
Rushton	5.5	5.38	0.98
6 Blade Paddle	4.5	4.68	1.04

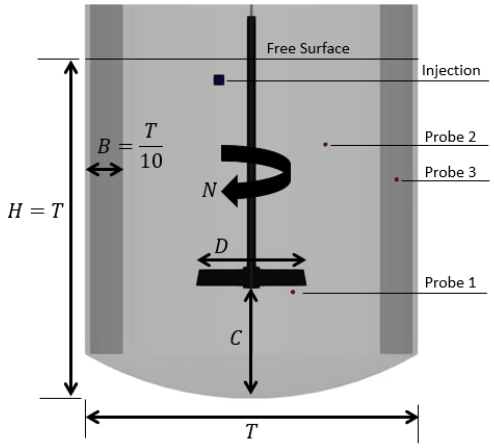

Figure 5. Vessel Layout for Mixing Simulations

Turbulent Free Jet

The software performed simulations of a turbulent free jet. The following parameters were used for this simulation: a liquid density of 1 g/mL, a liquid viscosity of 1 cP, a nozzle velocity of 5 m/s, and a nozzle diameter of 0.1 m. The Reynolds number is ~ 500,000. Because of the memory of the computer used for the simulations, the size of the geometry simulated had to be limited. The geometry simulated was a box that was 10 m long, 1 m wide, and 1 m high. The jet nozzle length was 2 m. Because of the closeness of the boundaries, the M-Star generated turbulent jet was only compared with data and correlations to a distance of 3 meters. At distances greater than 3 meters, the boundaries interfered with jet development. Because a turbulent jet takes approximately 6 nozzle diameters to be fully developed, no comparisons were made at a distance less than 6 nozzle diameters.

The velocity decay along the jet centerline was compared with data from Kiser and correlations from the technical literature.[8, 9] Equation [12] describes the jet centerline velocity as a function of distance from the jet origin

$$V/V_0 = C\ (D/x) \qquad [12]$$

where V_0 is the nozzle velocity, D is the nozzle diameter, x is the distance from the nozzle, and C is a constant.[10] Equation [12] is valid for x/D > 12. The value of C varies widely among researchers. Abramovich reports a value of 6.3, Blevins reports a value of 6 (with an uncertainty of 10%), Ball et al[11] reported values of 5.0 – 6.7 among various researchers. Shashidhara and Bourodimos reported values between 5.1 and 7.7.[12] In addition, some of the researchers use a virtual origin, which is different from the jet nozzle exit. Because of the wide variance in the values of C reported, the authors decided the best comparison for M-Star would be with the data from Kiser. Comparisons with equation [12] using values of 6.3 and 5.75 and Lee's simulations are included for information.

Figure 6 shows the centerline velocity of a turbulent free jet. The M-Star® simulation results agree with the Kiser[8] data and the Lee[10] CFD simulations to within 15%. Using a value of 6.3 for C, the M-Star® simulation results are within 30% of the predictions from equation [12] between x/D of 6 and 27. Using a value of 5.75 for C, the M-Star® simulation results are within 30% of the predictions from equation [12] between x/D of 6 and 29.

Another test for the M-Star® software is to compare the axial velocity as a function of the radial distance from the jet centerline. Equation [13] describes the relationship

$$V/V_{max} = \exp[-0.69\ (r/b)^2] \qquad [13]$$

where V_{max} is the axial velocity at the jet centerline, r is the radial distance from the jet centerline, and b is the radial distance from the jet centerline at which the velocity is half of the velocity at the centerline.[8,13] For a self-preserving turbulent free jet, equation [13] should not be affected by the axial distance from the jet origin. During the turbulent jet simulations, the axial velocity as a function of the radial distance from the jet centerline was calculated at distances of 1 m, 1.5 m, 2 m, and 2.5 m from the jet nozzle, which are distances which are not influenced by the jet core. The results are shown in Figure 6, along with the predictions from equation [13]. The results show the jet to be self-preserving, and to agree with previous work on turbulent free jets.

The test of the M-Star® software at simulating turbulent free jets is determined to be successful.

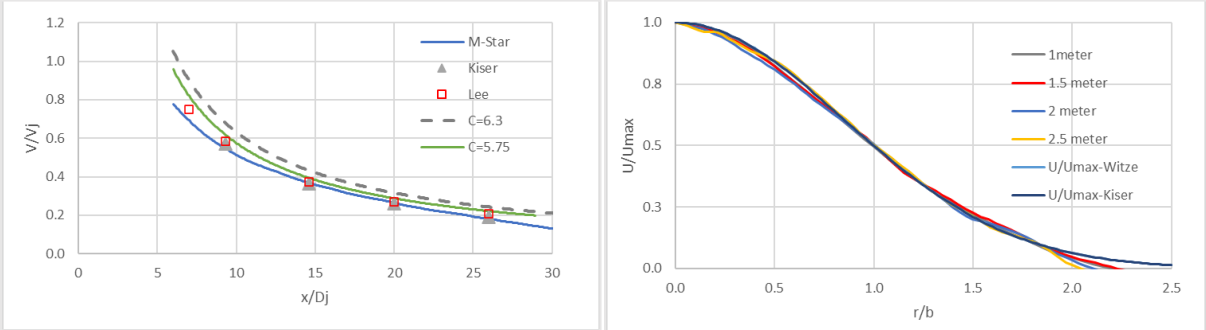

Figure 6. Centerline Axial Velocity of a Turbulent Free Jet (left) and Axial Velocity Profile (right)

Turbulent Pipe Flow Velocity Profile

The velocity profile during turbulent flow in a pipe does not have an analytical solution but has been well studied. The velocity profile is often fit with a function like the one shown in equation [14][2].[14,4,15]

$$V(r) = V_{max} (1 - r/R)^{1/n} \quad [14]$$

In equation [14], V(r) is the velocity as a function of radial position, V_{max} is the maximum velocity at the pipe center, r is the radial position, and R is the pipe radius. A value of 7 is often used for n.[14,4] Nikuradse investigated turbulent flow in rough pipes.[16] He also observed equation [14] to overpredict fluid velocity near the center of the pipe. A value of 7 will be used to compare with the M-Star® simulations.

Equation [14a] describes the relationship between V_{max} and n

$$V_{max} = V_{avg} [(n + 1) (2n + 1)/(2 n^2)] \quad [14a]$$

where V_{avg} is the average velocity across the pipe diameter.[15] If n is 7, V_{max} is 1.22 V_{avg}.

Turbulent pipe flow was simulated using M-star®, and the results compared with equation [14].

The following parameters were used for this simulation: a liquid density of 1 g/mL, a liquid viscosity of 1 cP, an inlet velocity of 0.2 m/s, a pipe diameter of 0.1 m, and a pipe length of 5 m. The Reynold number ($2 R v_{avg}/\nu$) is 20,000. Figure 7 shows the velocity profile across the pipe diameter at a distance of 4.5 m from the entrance, along with the velocity profile calculated in equation [14] using n = 7. Figure 7 shows the ratio of the M-Star® calculated velocity to the equation [14] calculated velocity across the pipe diameter. With a value of 7 for n, the ratio is between 87% and 103% across the pipe diameter, so the agreement is within 15%. The M-Star® simulations predict a flatter velocity profile in the center of the pipe than equation [14], which is consistent with Nikuradse's observation. The largest differences are observed near the wall where equation [14] loses its accuracy.[4] Numerically integrating the velocity across the pipe diameter, the flow rate in the M-Star® simulations is 0.00147 m^3/sec. Numerically integrating equation [14], the calculated flow rate is 0.00155 when n is 7. The difference is less than 6%.

[2] References 1 and 2 use a value of 7 for n, but no value is used in equation [14] to make it more general.

An additional simulation was performed with an inlet velocity of 0.5 m/s and a Reynolds number of 50,000. With a value of 7 for n, the ratio is between 88% and 111% across the pipe diameter, so the agreement is within 15%. The M-Star® simulations predict a flatter velocity profile in the center of the pipe than equation [14], which is consistent with Nikuradse's observation. The largest differences are observed near the wall where equation [14] loses its accuracy.[4] Numerically integrating the velocity across the pipe diameter, the flow rate in the M-Star® simulations is 0.00373 m^3/sec. Numerically integrating equation [14], the calculated flow rate is 0.00389 when n is 7. The difference is less than 5%.

Figure 7 shows some asymmetry in the velocity profile. This asymmetry likely results from the turbulence in the pipe flow and from M-Star® calculating a probability distribution for the fluid velocity.

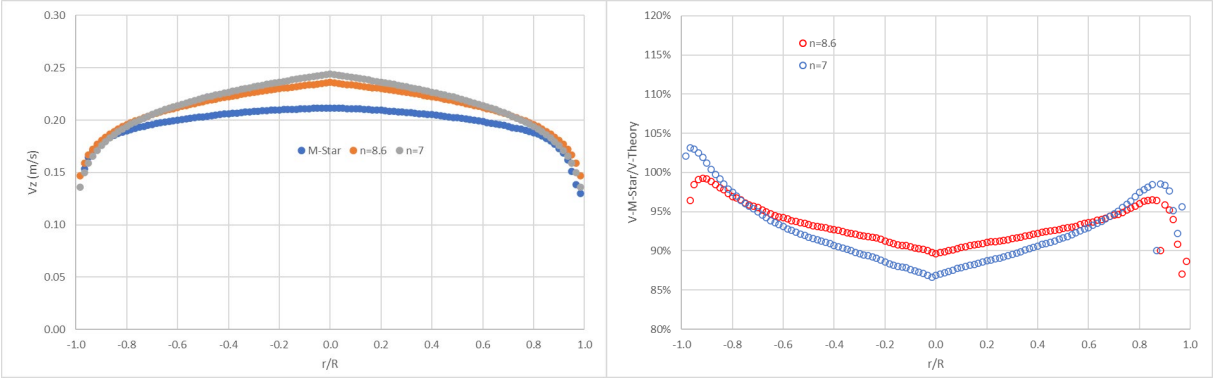

Figure 7. Velocity Profile in Smooth Pipe (left) and Comparison of Velocity Profile in Turbulent Pipe Flow with literature (right) at Reynolds Number of 20,000

Group 3

For Group 3, the authors selected four test problems to compare the M-Star® simulations with experimental data. The test problems are miscible liquid blending in a jet mixed tank, miscible liquid blending in an impeller mixed tank containing a non-Newtonian fluid, cavern mixing with an impeller in a tank containing a non-Newtonian fluid, and gas release from a Bingham plastic fluid in an impeller mixed tank. For the these problems, the acceptance criterion is to be within 30% of the literature data.

Cavern Mixing

Cavern mixing occurs in vessels with non-Newtonian fluids. Given that the DWPF SRAT and SME contain non-Newtonian (i.e., Bingham plastic) fluids, demonstrating the ability of the M-Star® software to simulate impeller mixing with non-Newtonian fluids will verify that it can simulate mixing in these vessels.

Although many constitutive relationships are available for describing the relationship between stress and strain in non-Newtonian fluids, one particularly general framework is the Herschel–Bulkley (HB) model:

$$\tau = K\dot{\gamma}^n + \tau_y \qquad [19]$$

where τ is the shear stress, $\dot{\gamma}$ is the shear rate, K is the consistency, n is the flow index, and τ_y is the yield stress.[17] If the HB model is parameterized using a zero-yield stress and a flow index equal to 1, it recovers the Newtonian (constant viscosity) model. If the HB model is parameterized using a zero-yield stress, it recovers the power-law fluid model. If parameterized with a non-zero yield stress but a flow index equal to 1, it recovers the Bingham plastic model. These last two parameterizations are particularly relevant to cavern mixing.

Simulations of cavern mixing were performed comparing cavern diameter with the empirical model developed by Elson et al (EN), and with experimental data from work done by Elson et al and Adams and Barigou.[18, 19] The EN model is an empirically developed model based on a right cylinder centered on and

coaxial with a Rushton impeller, with a height equal to 40% of the diameter and is described by equation [20]

$$(D_c/D)^3 = (1.36\ N_p/\pi^2)\ (\rho\ N^2\ D^2/\tau_y) \quad [20]$$

where D_c is the cavern diameter, D is the impeller diameter, N_p is the impeller power number, ρ is the fluid density, N is the impeller rotation speed, and τ_y is the fluid yield stress. This equation is applicable when the cavern diameter is larger than the impeller diameter but smaller than the tank diameter, i.e., when $D \leq D_C \leq T$. The EN model will only be compared to the M-Star® simulation where the cavern diameter is smaller than the tank diameter.

M-Star® Cavern Mixing Compared to Experimental Results from Elson

The experiments done to develop the EN model were modeled in M-Star® to confirm if M-Star® could yield the similar mixing caverns to Elson's original experiments.[18, 19] M-Star® derived cavern diameter, dimensionless cavern diameter, and cavern height to diameter ratio were compered to Elson's original experimental results. The cavern diameters calculated in M-Star® were determined by the maximum diameter across the cavern where the velocity is above 0.001 m/s after the system reaches steady state after 2 seconds and the maximum diameter in which a miscible scalar added near the impeller was well mixed in the fluid. The tank simulated in this comparison is a flat bottom tank with a diameter of 0.071 m meter with baffles. A Ruston turbine RBT with a diameter of 0.0355 meters was used so that the tests could be directly comparable to the 0.5 D/T experiments. The mixing speeds chosen were 480, 1020, and 1620 rpm to get caverns near the blade, between the blade and the wall, and at the vessel wall.

Elson originally described the rheology of the 3% xanthan gum solution, a yield stress fluid, used in the experiments using both the Casson and power law model.[18, 19] Unable to fit rheological models like the Herschel-Bulkley fluid model Elson used the Casson model to describe the fluid at low shear rates because it accurately described the yield stress. The power law fluid was used at higher shear rates above 0.09 s^{-1}. We were able to use Elson's original data to extract Herschel-Bulkley parameters using Microsoft excel as shown in Table IV below and the results show that our parameters yield rheological properties close to Elson's original data and models. It was necessary to find Herschel-Bulkley parameters in order to have the most accurate rheological model that has both a yield stress and accurately describes the rheology of the fluid at high shear rates to be used in the M-Star® model. The density of the fluid is 987 kg/m^3.

Table IV Rheological Parameters for Xanthan Gum

	Power Law	Casson	Herschel-Bulkley
Yield Stress (Pa)	n/a	20	11
K	40.3	2.73	28.5
n	0.143	n/a	0.195

The results of the experiment matched closely to those of Elson. The cavern diameters measured in M-Star® are all within 10% of those measured by Elson when using both velocity and miscible scalar to describe the mixing cavern as shown in Table V. The M-Star® measured cavern sizes using both velocity and miscible are within 10% of the experimental results in every case. Both velocity and miscible scalar were used as parameters to show how closely the two matched each other. The miscible scalar emulates what was done experimentally but takes more than 20 seconds of simulated time to mix to the edges of the cavern in some cases. The cavern fully develops and is steady within 5 seconds of simulated time in most cases so using velocity as a parameter for cavern diameter is much quicker than using a miscible scalar to determine cavern diameter.

The comparison of dimensionless cavern diameter as a function of Reynolds number was studied by Elson as a way to compare the experiments independent of the impeller diameter used.[18, 19] Dimensionless cavern diameter is the ratio of the cavern diameter to the diameter of the blade. Figure 8 A shows that the dimensionless cavern diameter measured in M-Star® closely matches those measured experimentally well within the target 30% threshold. Elson also studied the ratio of the cavern height to diameter and even used his results in developing the EN model.[18, 19] Elson found that when the cavern diameter is smaller than the vessel diameter the ratio of cavern height to diameter is between 0.35 and 0.45. The M-Star® miscible scalar results closely matched the experimental ratios shown in Figure 8 B since they recreated the scalar behavior of the dye in Elson's experiment. On the other hand, the M-Star® velocity ratios are larger than the experimental and scalar ratios. This is primarily due to the motion of the fluid in the middle of the vessel directly above the impeller. Although the fluid is in motion the miscible scalar will not travel to that region and become well mixed there. Overall M-Star® was able to proficiently model the mixing of this yield stress fluid with cavern diameters within 10% of experimental values.

Table V Comparison of results of Cavern mixing of Xanthan Solution from M-Star® and Literature

Impeller speed (rpm)	Re	N_p	D_C Elson (m)	D_C M-Star® (m) Velocity	D_C M-Star® (m) Scalar	D_C% difference Velocity	D_C% difference Scalar
480	11.1	14.7	0.043	0.045	0.044	5.0 %	2.3 %
1080	43.9	4.4	0.057	0.055	0.051	-3.2 %	-10.3 %
1620	102.3	1.7	0.071*	0.068	0.069	-4.6 %	-3.0 %

*The cavern has reached the wall of the vessel

Overall, the M-Star® data closely matched the experimental data and correlation values within the 30% criteria needed for this benchmark.

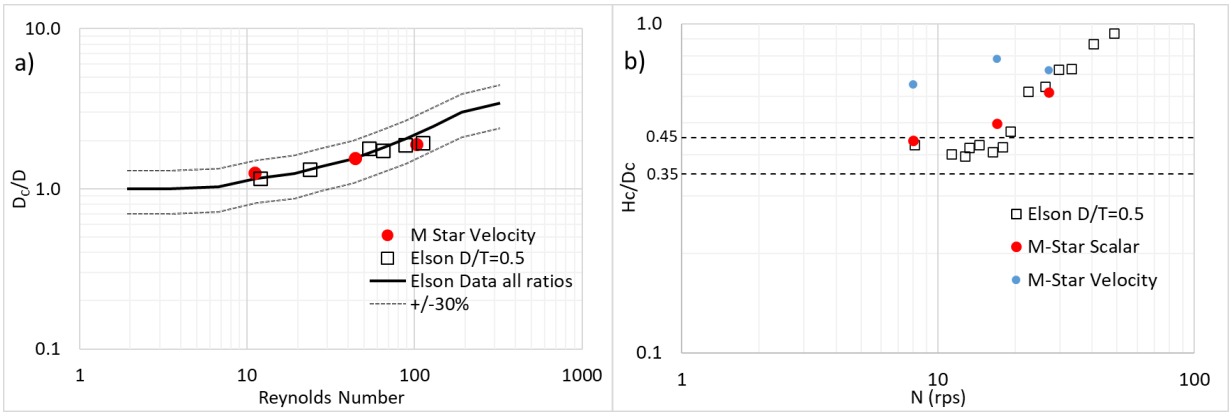

Figure 8 M-Star® results compared to experimental a) dimensionless cavern diameter as a function of Reynolds number b) cavern height to diameter ratio as a function of mixing speed

M-Star® Cavern Mixing Compared to Experimental Results from Adams

The use of models to predict cavern size comes with inherent uncertainties. Therefore, comparison between experimental data and M-Star® simulations were performed. The work performed by Adams and Barigou[19] was chosen as the experimental data. The 0.1% Carbopol solution used in the experiment was characterized as a Herschel-Bulkley fluid with the fluid properties shown in Table VI. The vessel used in M-Star® is the same as in the literature; vessel diameter of 0.148 m, 4 baffles of width 0.0148 m and thickness of 0.00148 m. The solution was agitated using a 6 bladed 45° down-pumping PBT with a diameter of 0.0493 m and an off-bottom clearance of 0.0493 m. The liquid height was 0.148 m. The lattice spacing for the M-Star® experiments modeled after the experiments performed by Adams and Barigou was 0.00074 m giving 200 lattice points across the diameter of the tank. The Courant number used was 0.001.

Table VI. Rheological properties of Carbopol solution

Re	Impeller speed (rpm)	N_p	Yield stress (Pa)	K (Pa s^n)	n	Density (kg/m^3)
7.3	69	12.3	2.625	0.541	0.555	997
20.4	95	4.7	1.413	0.373	0.572	997
70.3	194	2.8	1.289	0.348	0.573	997
86.6	246	2.7	1.558	0.446	0.551	997
163.2	372	2.1	1.966	0.373	0.583	997

The Adams and Barigou measured cavern diameters (D_C Adams) as stated in Table VI were found using planar laser induced fluorescence to visualize and measure the caverns.[19] The M-Star® cavern diameters are provided in Table VII and were determined from the M-Star® simulations where the steady state fluid velocity is greater than 0.001 m/s in the radial direction (D_C M-Star Velocity). The cavern diameter as determined by scalar (D_C M-Star Scalar) was determined by measuring the distance the scalar had traveled in the radial direction after mixing for an extended time between 20-40 seconds. In all cases the cavern diameter, when measured using fluid velocity, was constant after 2 seconds of simulated time as shown in Figure A-2. The percent difference between the M-Star® velocity and Adam's cavern diameters are within 20% in all cases.

The steady state velocity field and dye concentration for all cases between 20-40 seconds of agitation in M-Star® is shown in Figure 9. Longer times were needed for the scalar to fill the cavern at the higher mixing speeds. At this point, both the velocity and scalar (dye) concentration fields are stable and form a well-defined cavern. The fluid velocity inside the cavern shows a mixed fluid and is stagnant outside the cavern. The cavern profile generated by M-Star® using either the velocity or scalar field yields similar cavern diameter shapes, with larger differences in the height of the cavern. The M-Star® cavern result and the cavern profile measured by Adams and Barigou[19] at this same operation condition. Although the simulation appears to underpredict cavern formation just above the impeller, the overall shape and extent of the predicted cavern is in-line with the directly measured data.

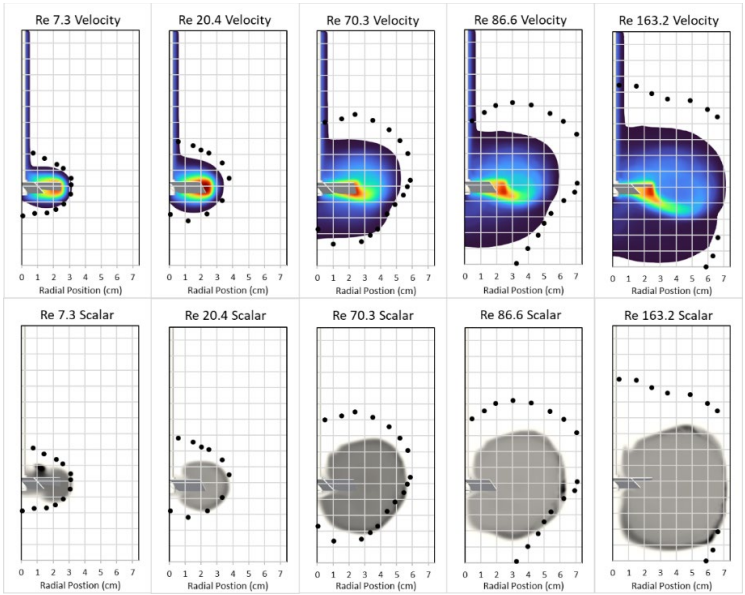

Figure 9. Comparing the predicted mixing cavern, as characterized using (top) velocity field and (bottom) scalar concertation, to the measured data (points)

Table VII. Comparison of results of Cavern mixing of Carbopol Solution from M-Star® and Literature

Re	D_C Adams	D_C M-Star Velocity	D_C M-Star Scalar	D_C EN	% dif Adams	% dif EN
7.3	0.062	0.064	0.067	0.063	3%	1%
20.4	0.074	0.071	0.077	0.070	5%	1%
70.3	0.117	0.108	0.114	0.097	8%	11%
86.6	0.148	0.12	0.129	0.105	19%	14%
163.2	0.148	0.144	0.148	0.118	3%	22%

The tests of cavern mixing are determined to be successful.

Blending with Non-Newtonian Fluid

Grenville measured the mixing time in an impeller mixed vessel containing non-Newtonian fluids.[20] He performed tests in vessels with diameters of 0.305, 0.609, and 1.83 m using pitch blade turbines, flat blade turbines, and hydrofoils. The fluids were pseudoplastics rather than Bingham plastics, but they are shear thinning fluids and will provide a good assessment of the software in simulating mixing of shear-thinning, non-Newtonian fluids. After the vessel mixing reached steady state, he added a miscible scalar and measured the concentration of the scalar as a function of time at three locations. When the concentration of the scalar at a probe was within 5% of the bulk concentration, the vessel was considered mixed at that probe location.

Figure 5 shows the tank layout, the position of the conductivity probes, and the location of the scalar addition. The probes are located underneath the impeller (center probe), halfway between the impeller shaft anf the tank wall (mid-way probe), and behind one of the baffles (baffle probe). Table VIII shows the parameters for these simulations.

Table VIII. Software Test Simulation Parameters

#	Tank Diameter (m)	Impeller Diameter (m)	Impeller Speed (rps)	Power Law constant (Ns^n/m^2)	n	Impeller
1	0.305	0.102	3.33	0.092	0.8	PBT
2	0.609	0.203	3.00	0.092	0.8	PBT
3	0.609	0.203	3.33	0.258	0.79	PBT
4	0.305	0.102	3.33	0.092	0.8	FBT
5	0.609	0.203	2.00	0.092	0.8	FBT
6	1.830	0.610	2.50	0.258	0.79	PBT
7	0.305	0.1525	3.67	0.092	0.8	Hydrofoil
8	0.609	0.203	4.00	0.258	0.79	FBT
9	0.609	0.203	2.92	0.068	0.86	FBT

Figure 10 shows a comparison of the measured blend time to the calculated blend time for each of the probes in each of the tests. With the exception of the baffle probe in tests 4 and 5, all of the M-Star calculated blend times are within 30% of the measured blend times. The tests of M-Star® simulations miscible liquid blending with non-Newtonian fluids are determined to be successful.

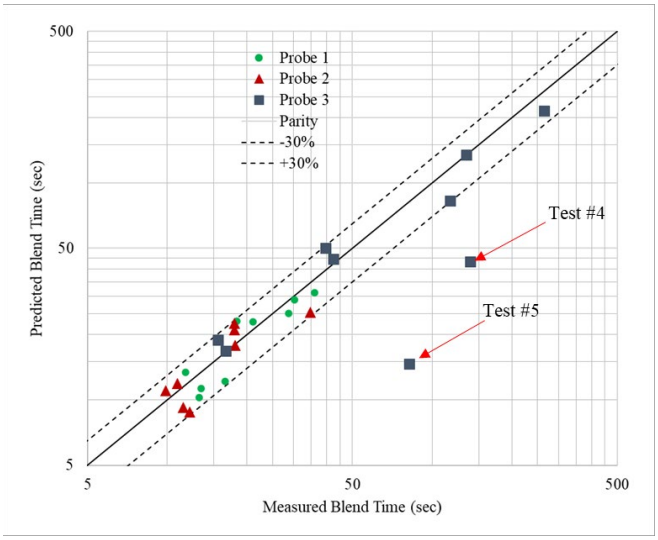

Figure 10. Parity Plot Comparing Measured Blend Time with M-Star Calculated Blend Time

Jet Mixed Tank

The objective of this task is to simulate the mixing of a jet mixed vessel with M-Star® and compare the mixing time results to mixing times of experimental data. In 1996 Grenville and Tilton performed various experiments of jet mixed tanks and developed a model to correlate the blend time data.[21, 22] The jet velocity, tank volume, tank fill height, and nozzle diameter were varied in these tests. For this study the 1.68 m diameter tank with a nozzle diameter of 26.1 mm was chosen to be modeled in M-Star®. Five simulations were done varying the jet velocity and the fluid height. The nozzle was aimed so that the jet would intersect the surface of the liquid at the opposite end of the tank and was adjusted depending on the liquid level. The recirculating outlet for the tank was located 45° from the nozzle along the edge of the tank. Grenville measured the blend times by injecting a pulse of 2.4 M sodium chloride solution into the vessel through the jet nozzle and the concentration was measured using 3 conductivity probes placed around the tank. The blend time is described as the time it takes the tracer to reach 99% homogeneity so that the concentration fluctuations are less than ± 1% the final concentration. For this experiment in M-Star® we injected a miscible scalar into the solution at the jet nozzle and used 3 probes placed in the same positions as Grenville did and measured the time it took for the root mean squared (RMS) concentration of these probes to reach 99% of the average concentration in the vessel. The RMS as defined by Grenville is described in Equation 17 where C is the miscible scalar concentration.[20]

$$C_{j,rms} = \left(\frac{1}{3}\left(C_{j,1}^2 + C_{j,2}^2 + C_{j,3}^2\right)\right)^2 \quad [21]$$

This case study is deemed successful if the blend times from M-Star® are within 30% of the values measured experimentally by Grenville. The results are shown below in Figure 11 where H/T is the ratio of the fluid height to the tank diameter and V is the jet velocity in m/s. The error bars are set to 30% of the value of the respective blend time and it can be seen that the M-Star blend times are all within 30% of the experimental values. In fact the M-Star® blend time values are all within 15% of the experimental values shown in Table IX.

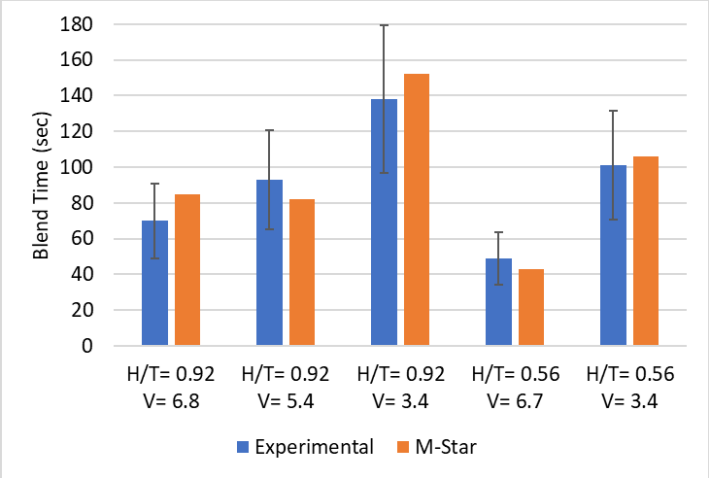

Figure 11 Experimental blending time results with 30% error bars compared to M-Star blending time results

Table IX Experimental blending times compared to M-Star blending time results

Case	Experimental Blend Time (s)	M-Star Blend Time (s)	% Difference
H/T= 0.92 V=6.8	70	77	10.0
H/T= 0.92 V=5.4	93	82	11.8
H/T= 0.92 V=3.4	138	152	10.1
H/T= 0.56 V=6.7	49	42	14.3
H/T= 0.56 V=3.4	101	114	12.9

The testing of the M-Star® software to simulate jet mixed tanks is determined to be successful.

CONCLUSIONS

The results of the Software Testing follow:

- The group 1 simulations were completed, and the simulation results agree with the analytical solutions to within 10%.
- The group 2 simulations were completed, and the simulation results agree with the well established solutions to within 20%.
- The group 3 simulations were completed, and the simulation results agree with the well established solutions to within 30%.

REFERENCES

1. Wright, I. M. G. *Continued Application of 13-Day Q-Time for Sludge Batch 9 Considering Retention Rate*; X-ESR-S-00292; SRMC: Aiken, SC, May 2020, 2020.
2. Wright, I. M. G. *DWPF Retained Hydrogen MSTAR Modeling*; X-TTR-S-00084, Rev. 1; Savannah River Remediation: Aiken, SC, May 2021.
3. Miedema, S. A. *Slurry Transport: Fundamentals, A Historical Overview and the Delft Head Loss and Limit Deposit Velocity Framework, Delft: S. A. Miedema*; Delft, 2016.
4. Bennett, C. O.; Myers, J. E., *Momentum. Heat, and Mass Transfer*. McGraw-Hill: New York, 1982.
5. Simpson, M. M.; Janna, W. S. *Newtonian and Non-Newtonian Fluids: Velocity Profiles, Viscosity Data, and Laminar Flow Friction Factor Equations for Flow in a Circular Duct*.
6. Ma, Z. Impeller Power Draw Across the Full Reynolds number Spectrum. University of Dayton.
7. Nagata, S.; Nishikawa, M.; Tada, H.; Hirabayashi, H.; Gotoh, S., Power Consumption of Mixing Impellers in Bingham Plastic Fluids. *J Chem Eng Jap* **1976,** *3* (2), 237 - 243.

8. Kiser, K. M., Material and Momentum Transport in Axisymmetric Turbulent Jets of Water. *AIChE Journal* **1963,** *9* (3), 386-390.
9. Abramovich, G. N., *The Theory of Turbulent Jets*. M.I.T. Press: Cambridge, MA, 1963.
10. Lee, S. Y.; Dimenna, R. A. *Fluent Test and Verification Document*; WSRC-TR-2005-00563, Rev. 1; SRNL: Aiken, SC, September 2006, 2006.
11. Ball, C. G.; Fellouah, H.; Pollard, A., The Flow Field in Turbulent Round Free Jets. *Progress in Aerospace Sciences* **2012,** *50*, 1-26.
12. Shashidhara, N. S.; Bourodimos, E. L., Turbulence and Diffusion Investigation in a Submerged Axisymetric water Jet. *Water Resources Bulletin* **1975,** *11* (1), 77-96.
13. Witze, P. O. *The Impulsively Started Incompressible Turbulent Jet*; SAND80-8617; Sandia Laboratories: October 1980.
14. Darby, R., *Chemical Engineering Fluid Mechanics*. 2nd Ed. ed.; Marcel-Dekker: New York :, 2001.
15. Blevins, R. D., *Applied Fluid Dynamics Handbook*. Van Nostrand Reinhold Company: New York, 1984.
16. Nikuradse, J. *Technical Memorandum 1292*; National Advisory Committee for Aeronautics: Washington, DC, 1950, 1950.
17. Acheson, D. J., *Elementary Fluid Dynamics*. Oxford University Press: 1990.
18. Elson, T. P.; Cheesman, D. J.; Nienow, A. W., X-Ray Studies of Cavern Sizes and Mixing Performance with Fluids Possessing a Yield Stress. *Chem. Eng. Sci.* **1986,** *41* (10), 2555-2562.
19. Adams, L. W.; Barigou, M., CFD Analysis of Caverns and Pseudo Caverns Developed During Mixing of Non Newtonian Fluids. *Chemical Engineering Research and Design* **2007,** *85* (5), 598-604.
20. Grenville, R. K. Blending of Viscous Newtonian and Pseudo-Plastic Fluids. Cranfield Institute of Technology, 1992.
21. Grenville, R. K.; Tilton, J. N., A New Theory Improves the Correlation of Blend Time Data from Turbulent Jet Mixed Vessels. *Trans IChemE* **April 1996,** *74 Part A*, 390-396.
22. Grenville, R. K.; Tilton, J. N., Jet mixing in tall tanks: Comparison of methods for predicting blend times. *Chem Eng Res Des* **2011,** *89* (12), 2501-2506.